Integrative Biology

PAPER

View Article Online
View Journal | View Issue

Cite this: *Integr. Biol.*, 2018, 10, 313

Chitosan nanoparticles' functionality as redox active drugs through cytotoxicity, radical scavenging and cellular behaviour†

Sreelatha Sarangapani, *[a] Ajeetkumar Patil, [ab] Yoke Keng Ngeow,[c] Rosmin Elsa Mohan,[d] Anand Asundi [d] and Matthew J. Lang*[ae]

Targeting the oxidative stress response has recently emerged as a promising strategy for the development of therapeutic drugs for a broad spectrum of diseases. Supporting this strategy, we have reported that chitosan nanoparticles synthesized with a controlled size had selective cytotoxicity in leukemia cells through the mechanism related to reactive oxygen species (ROS) generation. Herein, we found that the cellular uptake of chitosan nanoparticles was enhanced in a time dependent manner and inhibited the cellular proliferation of leukemia cells in a dose dependent manner with elevation of the reactive oxygen species (ROS) showing a stronger effect on apoptosis, associated with the upregulation of caspase activity and the depletion of reduced glutathione. Propidium iodide and calcein staining demonstrated the central role of the chitosan nanoparticles in triggering elevated ROS, inducing cell death and intracellular oxidative activity. The enhanced free radical scavenging activity of the chitosan nanoparticles further iterates its antioxidant activity. *In vitro* quantitative phase imaging studies at the single cell level further demonstrated the inhibition of cellular proliferation with significant changes in cellular behavior and this supported our hypothesis. Hemocompatibility tests demonstrated that chitosan nanoparticles could be used safely for *in vivo* applications. Our findings suggest that chitosan nanoparticles may be a promising redox active candidate for therapeutic applications.

Received 28th February 2018,
Accepted 6th April 2018

DOI: 10.1039/c8ib00038g

rsc.li/integrative-biology

Insight, innovation, integration

Chitosan nanoparticles have gained significant importance as a sustainable natural product for complementary and alternative therapy. Despite the progress of chitosan nanoparticles in biomedical science there is still a knowledge gap on their therapeutic efficiency and interaction with cellular behavior. This manuscript is about the biocompatibility and toxicity of chitosan nanoparticles in a cellular environment. Chitosan nanoparticles interact with leukemia cells and modify the cellular behavior with dose dependent cytotoxicity. Our study demonstrates the emergence of chitosan nanoparticles for the sustainable development of redox active drugs at the molecular level, inducing cell death and intracellular oxidative activity. This research deepens the understanding of chitosan nanoparticles that target the oxidative stress response for therapeutic efficacy and sustainable use. Therefore, this study explores the potential biological impact of chitosan nanoparticles in a cellular microenvironment as redox regulators.

Introduction

Chitosan, a natural polysaccharide, is gaining attention in the pharmaceutical field due to its significant properties like biodegradability, biocompatibility, bioactivity and polycationicity. It is obtained by the *N*-deacetylation of chitin and is widely used in the development of new therapeutic drug delivery systems, nanomedicine and biomedical engineering. It is a multipurpose biomaterial and in acidic aqueous solution chitosan oligomers self-assemble to form nanoparticles *via* cross-linking.[1] Chitosan nanoparticles with their widespread applications in drug delivery vehicles have been shown to exert anti-cancer effects against several types of cancer. With the limited therapeutic

[a] *Biosystems & Micromechanics (Biosym) IRG, Singapore MIT Alliance for Research & Technology (SMART), Singapore. E-mail: sree09latha@gmail.com, matt.lang@vanderbilt.edu*
[b] *Department of Atomic and Molecular Physics, Manipal Academy of Higher Education, Manipal, India*
[c] *Department of Biological Science, National University of Singapore, Singapore*
[d] *School of Mechanical and Aerospace Engineering, Nanyang Technological University, Singapore*
[e] *Department of Chemical and Biomolecular Engineering and Department of Molecular Physiology and Biophysics, Vanderbilt University, Nashville, TN 37235, USA*

† Electronic supplementary information (ESI) available. See DOI: 10.1039/c8ib00038g

efficacy of chemotherapeutic agents and cell resistance to multiple anticancer drugs, chitosan nanoparticles appear to exhibit great potential for cancer treatment due to their small size, varied composition, surface functionalization and stability which provides unique opportunities to interact with and target the tumor microenvironment.[2]

Current therapeutic strategies which involve a combination of surgical resection, radiation therapy and chemotherapy pose a huge risk of an inability to administer therapeutic agents selectively to the targeted sites, without adverse effects on healthy tissue.[3] Considered as a viable alternative to conventional chemotherapeutic drugs, the interactions of chitosan nanoparticles with the tumor aid small molecular transport to the intracellular organelles to induce the greatest cytotoxic effect, which targets cells selectively. As a functional biopolymer, it elicits dose-dependent inhibitory effects on the proliferation of various tumor cell lines, while having low toxicity against normal human cells.[4]

With its unique characteristic nontoxicity, chitosan is one of the abundant and renewable carbohydrate polymers available largely in the exoskeletons of shellfish and insects. Chitosan can act on tumor cells directly to interfere with cell metabolism, inhibit cell growth and improve the body's immune function.[5] The positive charges on chitosan have a selective adsorption and neutralizing effect on the tumor cell surface and play a crucial role in antioxidant defence and redox regulation. The mechanism of the oxidative stress mediated ROS generation therapy that selectively kills cancer cells is gaining acceptance having physiological relevance.[6] With this in mind, the pivotal role of chitosan nanoparticles in the antioxidant defence mechanism has to be explored in detail. With the controlled size synthesis of nanoparticles, the interactions between chitosan nanoparticles and chitosan on leukemia cells were evaluated to ensure its scavenging activity, by reducing the generation of cancerous lesions. Therefore the goal of the present study was to explore the mechanism of the ROS mediated effect of chitosan nanoparticles on leukemia cell generation in comparison with that of the chitosan polymer. To illustrate the possible mechanism of the chitosan nanoparticles we studied the cytotoxicity, hemolytic activity, free radical scavenging activity and cellular behavior. To further demonstrate that chitosan nanoparticles can induce the production of reactive oxygen species (ROS) in cancer cells we investigated the level of intracellular oxygen species and the antioxidant activity. Such measurements provide additional insight into the molecular understanding of cancer and the effect of drug treatment.

Experimental section

Reagents and cell culture

Acetic acid, low molecular weight chitosan (LMW CS) (85% degree of deacetylation) and sodium tripolyphosphate (TPP) were purchased from Sigma-Aldrich Co. (MO, USA). The human T lymphocyte acute T cell leukemia BCL2 (AAA) Jurkat (ATCC® *CRL-2902*™) and human embryonic kidney cells (HEK 293, ATCC® *CRL-1573*) were purchased from American Type Culture Collection (ATCC), USA. Cells were maintained in RPMI 1640 medium supplemented with 10% FBS and 200 μg mL^{-1} G418 at 37 °C in a humidified atmosphere of 5% CO_2. All of the experiments were carried out in accordance with the relevant guidelines. The blood collection procedure was verified and approved by the Institutional Review Board (IRB-2017-03-020) of Nanyang Technological University (NTU).

Synthesis of chitosan nanoparticles

Chitosan nanoparticles (CSNPs) were prepared using an ionic gelation method.[7] Chitosan nanoparticles were obtained by adding chitosan solution to sodium tripolyphosphate (TPP) solution and incubating for 5 minutes followed by centrifugation for 1.5 hours at 16 000*g*. The supernatant was discarded and the resulting pellet was re-suspended in distilled water containing 0.1 M acetic acid by vortexing. The suspension was centrifuged for 45 minutes at 16 000*g* and the top 500 μL was freeze dried and the lyophilized powder was then used for further experimentation.

Determining the size and charge of CSNP by dynamic light scattering

The nanoparticles' size and zeta potential were measured using a Nano Zetasizer® (Malvern Instruments, UK) by a dynamic light scattering technique. The absorbance used was 0.001 as recommended in the Zetasizer UV user manual and the refractive index used was 1.590.[8]

FTIR characterization

The FTIR spectra of the chitosan nanoparticles and each of the individual components, chitosan and TPP, were obtained using a potassium bromide (KBr) method in the range of 400 cm^{-1} to 4000 cm^{-1}. A total of 16 readings were carried out for each run. The potassium bromide pellet was made with a sample of KBr at a ratio of 1 : 200. The final readings were obtained after the system stabilized for at least 20 minutes after loading the sample to ensure there was a low level of moisture in the chamber.

TEM imaging

The morphology of the nanoparticles was examined using transmission electron microscopy. About 20 μL of the chitosan nanoparticle solution was dropped on a carbon-coated copper mesh and air-dried for at least 1 hour at room temperature without using any stain. TEM images were obtained from a JEOL JEM-2010F model Field Emission Electron Microscope.

Synthesis of FITC-labelled CSNPs and the cellular uptake of CSNPs

FITC-labelled CSNPs were obtained using the method described by Masarudin *et al.*[9] The conjugation of FITC to chitosan was done by adding FITC solution to chitosan solution. After mixing well the TPP solution was added to the chitosan–FITC solution. The cellular uptake of the chitosan nanoparticles was visualized using fluorescence microscopy at different time intervals over a period of time.

Cell viability assay

An MTT assay was performed with a cell density of 2×10^4 cells per well. The volume of cells added to each well was fixed at 100 μL. The cells were treated with 0.2% DMSO (vehicle control) and chitosan and chitosan nanoparticles at (10–50 μg mL^{-1}) for 48 h under the same conditions. Both treatment and control groups were prepared in 6–8 replicate wells. The relative number of viable cells was then determined 24 h after incubation by adding 1 mg mL^{-1} of 3-[4,5-dimethylthiazol-2-yl]-2,5-diphenyl tetrazolium bromide (MTT) and incubating for a further 4 h. The formazan crystals formed were then solubilized with acidified isopropanol for 1 h. The absorption value of the solution at 595 nm directly represents the relative cell numbers. The cell decrease percentage relative to the control group was then determined.[10] The percentage of cell viability was calculated according to the following equation.

$$\%\ \text{of cell viability} = \text{absorbance of treated cells/absorbance of control cells} \times 100$$

Live/dead staining

Each well in the 96 well plate was seeded with 5×10^5 cells with the addition of chitosan nanoparticles or chitosan with varying concentration. Calcein and propidium iodide were added to each well at time point $t = 0$ min. The intracellular esterase in live cells converts cell permeable non-fluorescent calcein dye to fluorescent calcein dye, hence allowing the assessment of cell viability. Calcein exhibits green fluorescence detected at 520 nm with an excitation wavelength of 490 nm. On the other hand, propidium iodide is impermeable to the intact cell membrane of viable cells but it is able to enter dead cells with a porous membrane to intercalate with nucleic acid to give a fluorescence signal, allowing the assessment of cell death. Propidium iodide exhibits red fluorescence detected at 619 nm with an excitation wavelength of 535 nm.[11]

Caspase assay

Each well in the 96 well plate was seeded with 5×10^5 cells. Both chitosan and chitosan nanoparticles were added at a concentration of 50 μg mL^{-1}. Cells containing only media served as the negative control. CellEvent™ Caspase-3/7 Green Detection Reagent was added to each well at time point $t = 0$ min. The green fluorescence was detected at 530 nm when the sample was excited at 503 nm. A fluorescence signal was detected at a time point of 30 minutes, 60 minutes, 120 minutes and 240 minutes.[12]

Reactive oxygen species assay

Intracellular reactive oxygen species (ROS) production[13] was measured in both treated and control cells using dichlorodihydro-fluorescein diacetate (DCFH-DA). Briefly 2×10^4 cells per well were exposed to chitosan nanoparticles and incubated. After incubation, treated and control cells were resuspended in 0.5 mL PBS containing DCFH-DA at 37 °C for 30 min and then incubated with 4 mM H_2O_2 at 37 °C for 30 min. The ROS production of the cells was evaluated by a microplate reader (Perkin-Elmer, MA).

Total cellular GSH

Reduced glutathione (GSH)[14] is measured by its reaction with DTNB (5,5′-dithiobis nitro benzoic acid) to give a yellow colored compound that absorbs at 412 nm. A GSH assay kit (Sigma Aldrich) was used for evaluating the total cellular GSH.

DPPH scavenging activity

The ability of the nanoparticles to bleach 1,1-diphenyl-2-picrylhydrazyl (DPPH)[15] can be quantified using a spectrophotometric assay, the extent of scavenging causing a proportionate change in the absorption at 518 nm. An exact amount of the methanolic solution of DPPH was added with different concentrations of the nanoparticles and allowed to stand at room temperature for 30 minutes. Methanol served as the blank. After 30 minutes, the absorbance was measured at 518 nm and converted into the percentage of radical scavenging activity as follows:

$$\text{Scavenging activity (\%)} = A_{518}[\text{control}] - A_{518}[\text{sample treated}]/A_{518}[\text{control}] \times 100$$

Hydroxyl radical scavenging activity

The hydroxyl radical scavenging activity[16] was determined by a deoxyribose method. The damage to deoxyribose was quantified with a thiobarbituric acid reactive substance which can be taken as a measure of hydroxyl radical scavenging activity. The reaction mixture contained 2.8 mM deoxyribose, 0.1 mM $FeCl_3$, 0.1 mM EDTA, 1 mM H_2O_2, 0.1 mM ascorbate and 20 mM KH_2PO_4–KOH buffer (pH 7.4), and 20 μL of chitosan nanoparticle solution was added to the final volume of the reaction mixture. Then the reaction mixture was incubated for 1 hour at 37 °C. Then 1% of TBA was added and heated in a boiling water bath for 20 minutes. The pink colour produced was measured at 535 nm using a microplate reader. Deoxyribose degradation was measured as TBARS and the percentage of inhibition was calculated.

$$\text{Scavenging activity (\%)} = A_{535}[\text{control}] - A_{535}[\text{sample treated}]/A_{535}[\text{control}] \times 100$$

In vitro measurements of chitosan nanoparticles for hemocompatiblity

Hemolytic assay. Fresh human whole blood was anticoagulated and centrifuged, then washed with phosphate buffered saline (PBS, pH 7.4) to completely remove the serum following standard procedures. The separated red blood cells were suspended with the PBS solution. To 0.2 mL of human red blood suspension deionized water was added as the negative control or PBS solution as the positive control. Both the chitosan and chitosan nanoparticle solution at a concentration of 50 μg mL^{-1} were added to the human red blood cell suspension with the PBS solution and further incubated for 2 h at 37 °C and then

centrifuged at 10 000 rpm for 3 min. The optical density of the supernatant was measured at 540 nm using the microplate reader. The percentage of hemolysis[17] was calculated using the following equation.

$$\text{Hemolysis (\%)} = \text{Abs}_{540}[\text{sample treated}] - \text{Abs}_{540}[\text{negative control}]/\text{Abs}_{540}[\text{positive control}] - \text{Abs}_{540}[\text{negative control}] \times 100.$$

Morphological analysis. Blood smear tests were performed with chitosan and chitosan nanoparticles at a concentration of 50 μg mL^{-1}. The influence of chitosan and chitosan nanoparticles on the morphology of the RBCs was analyzed and used to differentiate between the normal and abnormal cells.

Characterizing cell metrics by phase measurement

The d'Bioimager imaging system[18] uses a transport of intensity equation to extract the phase from three or more images in focus. The phase retrieved is simulated as a stack to study morphological changes. It replaces a standard camera for any bright field microscope and provides 3D and 4D images of live cells. The d'Biomager retrieves a quantitative phase and hence an optical depth based on the Transport of Intensity Equations (TIE). By acquiring the three frames in rapid succession, it provides real-time quantitative phase imaging (3D) over time (4D). The novel optics and algorithm allow for near real-time measurement of phases in leukemia cells with chitosan biopolymer and chitosan nanoparticles and also in RBCs under the same treatment conditions which can add further clarity to the physical changes associated with cytotoxicity and biocompatibility.

Statistical analysis

Statistical analysis was performed using a Student's *t*-test and only the *p*-values of the samples that showed significant differences were reported. (* indicates a significant difference ($p < 0.05$) compared to the control.) Data are represented as the mean value ± S.D. of three or six independent replicates for each experiment ($n = 3$ or 6).

Results & discussion

Characterization of chitosan nanoparticles

Chitosan nanoparticles (CSNPs) were synthesized by an ionic gelation method by cross linking tripolyphosphate with chitosan (Fig. 1). Cross linking reduces the availability of the free amino groups on chitosan and prevents self aggregation. The average size of the chitosan nanoparticles obtained were ≤100 nm determined by randomly counting 200 particles on the TEM images (Fig. 2a) and by using a nanozetasizer. The particles synthesized were homogenously dispersed with low polydispersity index (PDI) values. The interaction between the chitosan chains and tripolyphosphate was evidenced by the FT-IR spectrum of the chitosan nanoparticles compared with that of native chitosan. The stretching modes of the O–H and N–H bonds in the chitosan matrix were attributed to a broad peak between 3350 and 3270 cm^{-1} which shifts to lower wavenumbers indicating hydrogen bond interactions.[19] The other peaks observed were those of the P–O stretching at 1201 cm^{-1} and P–O bending at 885 cm^{-1} of TPP. These results were consistent with the previously published data[20] (Fig. S1, ESI†). Colloidal system stability is directly proportional to the magnitude of the surface charge by the electrostatic repulsion between the particles.[21] The mean zeta charge for the pure chitosan nanoparticles was around +40.5 mV implying its efficiency which is directly proportional to the electrostatic interactions.[22] The polydispersity index indicates nanoparticle stability and its uniformity. The lower value of PDI (0.300 ± 0.027) for chitosan nanoparticles indicates the higher particle stability and the formation of nanoparticles with a controlled size. The application of chitosan nanoparticles that modulate the acute T cell leukemia and provide a synergy of action is represented in the scheme shown in Fig. 2b.

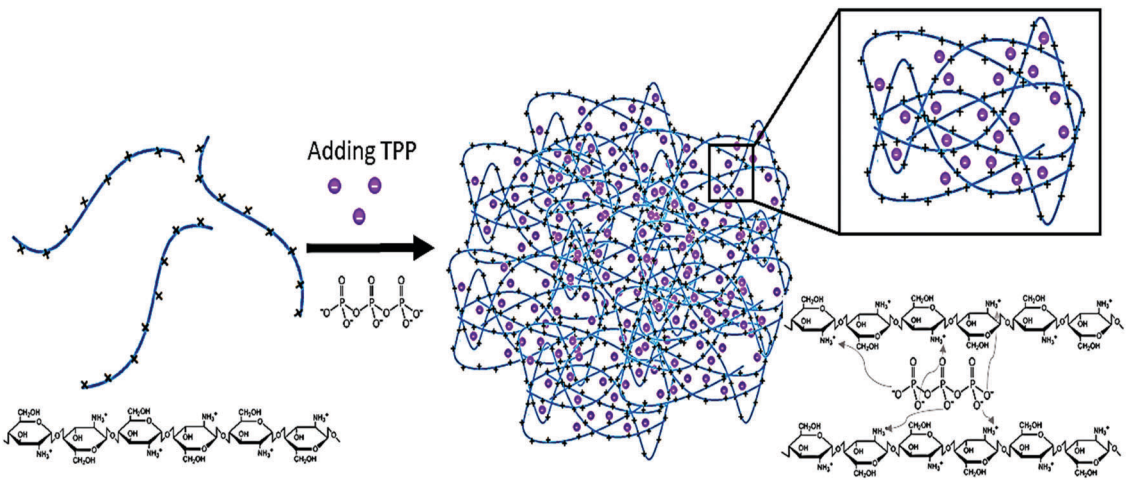

Fig. 1 The formation of chitosan nanoparticles. The chitosan nanoparticles are formed *via* crosslinking between the positively charged TPP and negatively charged chitosan polymers.

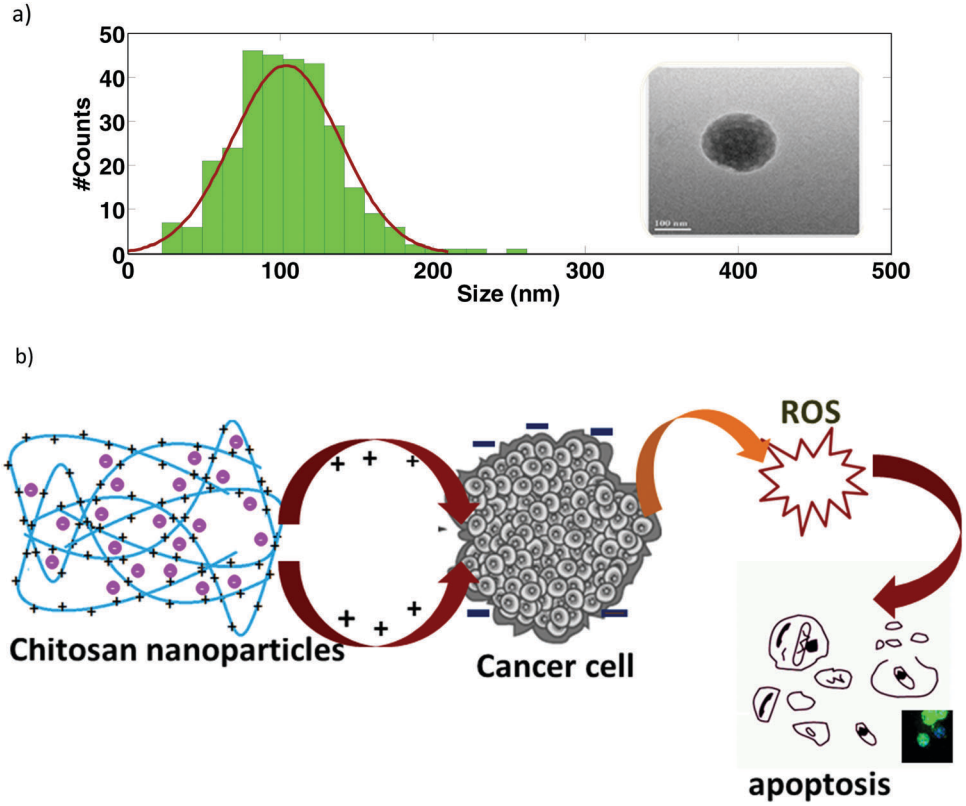

Fig. 2 (a) The TEM images of chitosan nanoparticles and their distribution. (b) A representation of chitosan nanoparticles leading to membrane disruption and the induction of cytotoxicity.

Cellular uptake of chitosan nanoparticles

To determine the effects of chitosan nanoparticles and to investigate the enhanced particle accumulation in the cells the nanoparticles were fluorescently labeled with FITC. For time dependent cellular uptake, acute lymphoblastic leukemia cells (Jurkat cells) were treated with FITC labeled chitosan nanoparticles and viewed at specific time intervals. For control cells, human embryonic kidney cells were also treated with FITC labeled chitosan nanoparticles and viewed at specific time intervals. The results indicated that intracellular nanoparticle uptake occurred as early as 30 minutes post cell treatment and were visualized as green dots using fluorescence microscopy. A similar fluorescence was not observed in the control cells without the treatment. The significant uptake of nanoparticles was observed 4 h post treatment along with stronger fluorescence intensity (Fig. S2, ESI†). The uptake was significantly increased 24 h post treatment with higher fluorescence intensity. Generally by increasing the time after nanoparticle exposure, uptake increases. This is evident in the Jurkat cells which show a time dependent increase in fluorescence intensity. In human

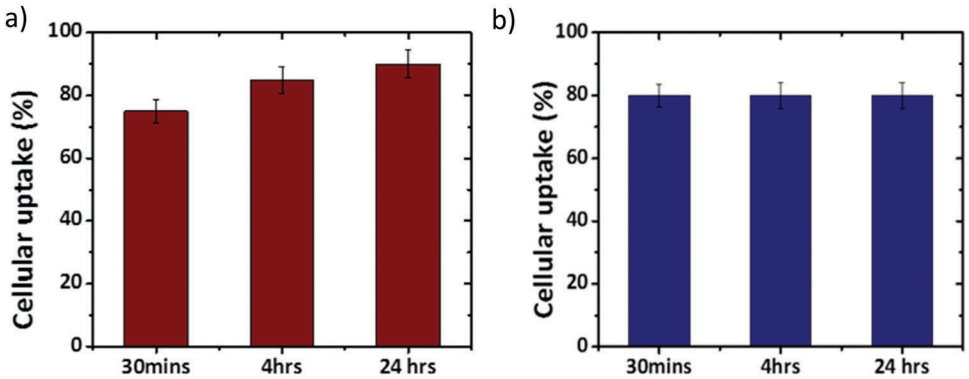

Fig. 3 The cellular uptake of FITC-labelled chitosan nanoparticles. (a) The percentage of cellular uptake quantified by the number of FITC positive cells in acute lymphoblastic leukemia cells. (b) The percentage of cellular uptake quantified by the number of FITC positive cells in human embryonic kidney cells. Data are represented as the mean value ± S.D. of three independent replicates (n = 3).

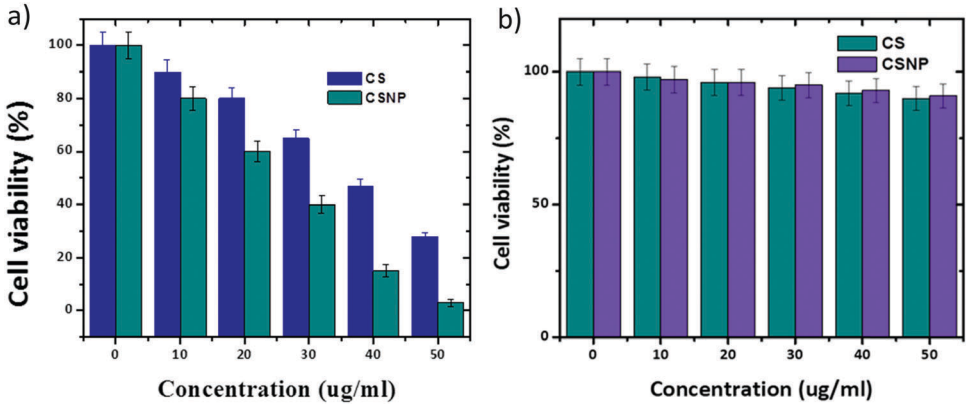

Fig. 4 The cytotoxic effects of chitosan and chitosan nanoparticles on (a) acute lymphoblastic leukemia cells and (b) human embryonic kidney cells after 24 h. Analysis of the MTT assay results showed that there was a time-dependent decrease in the viability of acute lymphoblastic leukemia cells when treated with chitosan nanoparticles and chitosan, and with human embryonic kidney cells it showed viability both with chitosan nanoparticles and chitosan. Data are represented as the mean value ± S.D. of three independent replicates (n = 3).

embryonic kidney cells (Fig. S3, ESI†) there was a mean fluorescence intensity which was stable over time. This stable increase could be due to the cellular heterogeneity. Meanwhile cancer cells display a high metabolic rate which may account for the higher uptake. This enhanced particle accumulation also supports our results from the previous related reports.[23] Therefore, from the results shown in Fig. 3, it could be suggested that nanoparticle cellular uptake follows a time dependent increase which follows either an endocytosis based pathway or a fluid-phase uptake mechanism.[24]

Cellular cytotoxicity of CSNPs

The effect of chitosan nanoparticles on cellular viability was calculated by the MTT assay. The leukemia cells were treated with different concentrations of the chitosan nanoparticle and chitosan and assessed for cell viability (shown in Fig. 4). The cytotoxicity of the chitosan nanoparticles implies that there will be alterations to the percentage of cell viability in the treated cells. The IC_{50} value was found to be 10 μg mL^{-1} for the acute leukemia cells after 24 h. But at a higher concentration of 50 μg mL^{-1} the chitosan nanoparticles inhibited the cell viability of the leukemia cells significantly. The highly positively charged amino groups in the chitosan molecule are attracted to the cancer cell membrane, which has a greater negative charge than that of normal cells. Thus the chitosan nanoparticles can act on tumor cells directly to interfere with cell metabolism, inhibit cell growth or induce cell apoptosis.[25] The significant decrease of cell viability evidenced by the higher potential of the chitosan nanoparticles than that of the chitosan polymer interrupts the action of the mitochondrial dehydrogenase with elevation of the ROS, which in turn is responsible for the cytotoxicity at

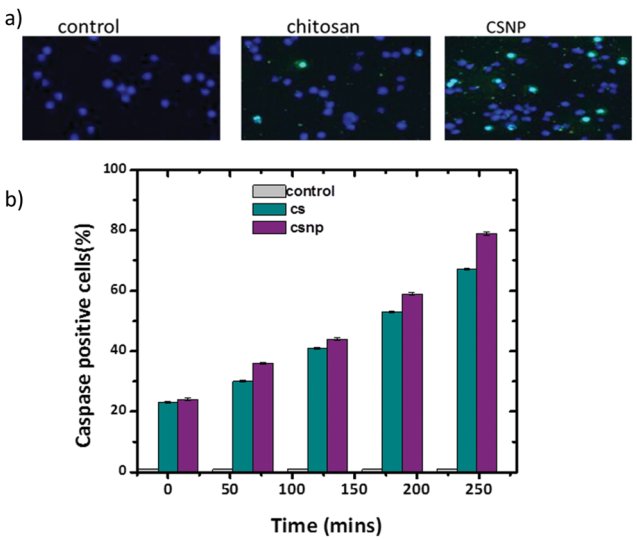

Fig. 5 (a) The detection of apoptosis in acute lymphoblastic leukemia cells at 40× magnification by confocal imaging. The apoptosis event was examined after exposure to the control only, 50 μg mL^{-1} chitosan & 50 μg mL^{-1} CSNPs at 240 minutes. (b) Cells incubated with media only served as the negative control. Cells stained green indicate caspase activity for 50 μg mL^{-1} chitosan & 50 μg mL^{-1} CSNP after 240 minutes of treatment. Data are represented as the mean value ± S.D. of three independent replicates (n = 3).

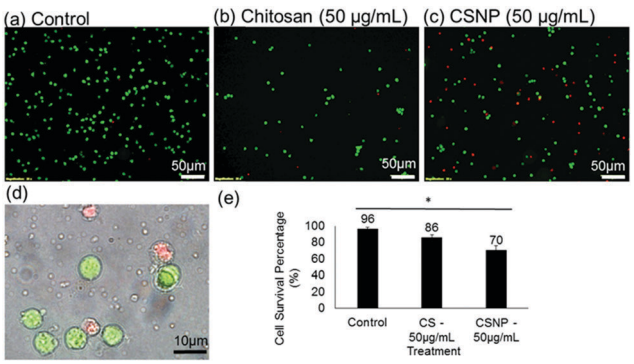

Fig. 6 The effect of chitosan and nanoparticles in acute lymphoblastic leukemia cells. (a) The survival of the cells incubated with media only was equivalent to (b) the cells treated with 50 μg mL^{-1} chitosan for 2 hours. (c) The cells showed a loss in viability after incubation with 50 μg mL^{-1} chitosan nanoparticles for 2 hours. (d) The morphology of the dead and viable cells. (e) The cell survival percentage determined quantitatively shows that the CSNPs decrease cell survival. Data are represented as the mean values ± S.D. of three independent replicates. (* indicates a significant difference ($p < 0.05$) compared to the control.)

higher concentrations. Thus the conclusion regarding the cytotoxic mechanism can be supported by the cell viability and caspase assay. The results also explain its pro-oxidant activity and demonstrate the therapeutic application of the chitosan nanoparticles as a chemotherapeutic agent.[26] With human embryonic kidney cells there was no change in the cell viability both with chitosan and chitosan nanoparticles which confirms its biocompatible nature.

Caspase activity

Caspases are aspartate-directed cysteine proteases synthesized as inactive precursors that cleave a diverse group of intracellular substrates to contribute various manifestations of apoptosis. They are activated as a consequence of signalling induced by a wide range of physiological and pathological stimuli and the response is both time and concentration dependent.[27] For cells treated with chitosan and CSNPs, the percentage of caspase-positive cells increased to 65% and 70% respectively after 4 hours of treatment (shown in Fig. 5). The percentage of caspase-positive cells is highest at 240 minutes after incubation with chitosan and CSNPs. The percentage of caspase-positive cells was higher for cells treated with 50 μg mL^{-1} of chitosan nanoparticles than with 50 μg mL^{-1} of chitosan. Our data supports the findings that chitosan nanoparticles trigger caspase activation with elevation of the ROS in the acute lymphoblastic leukemia cells in a dose dependent manner and over time that they eventually trigger programmed cell death as denoted by the green fluorescence.

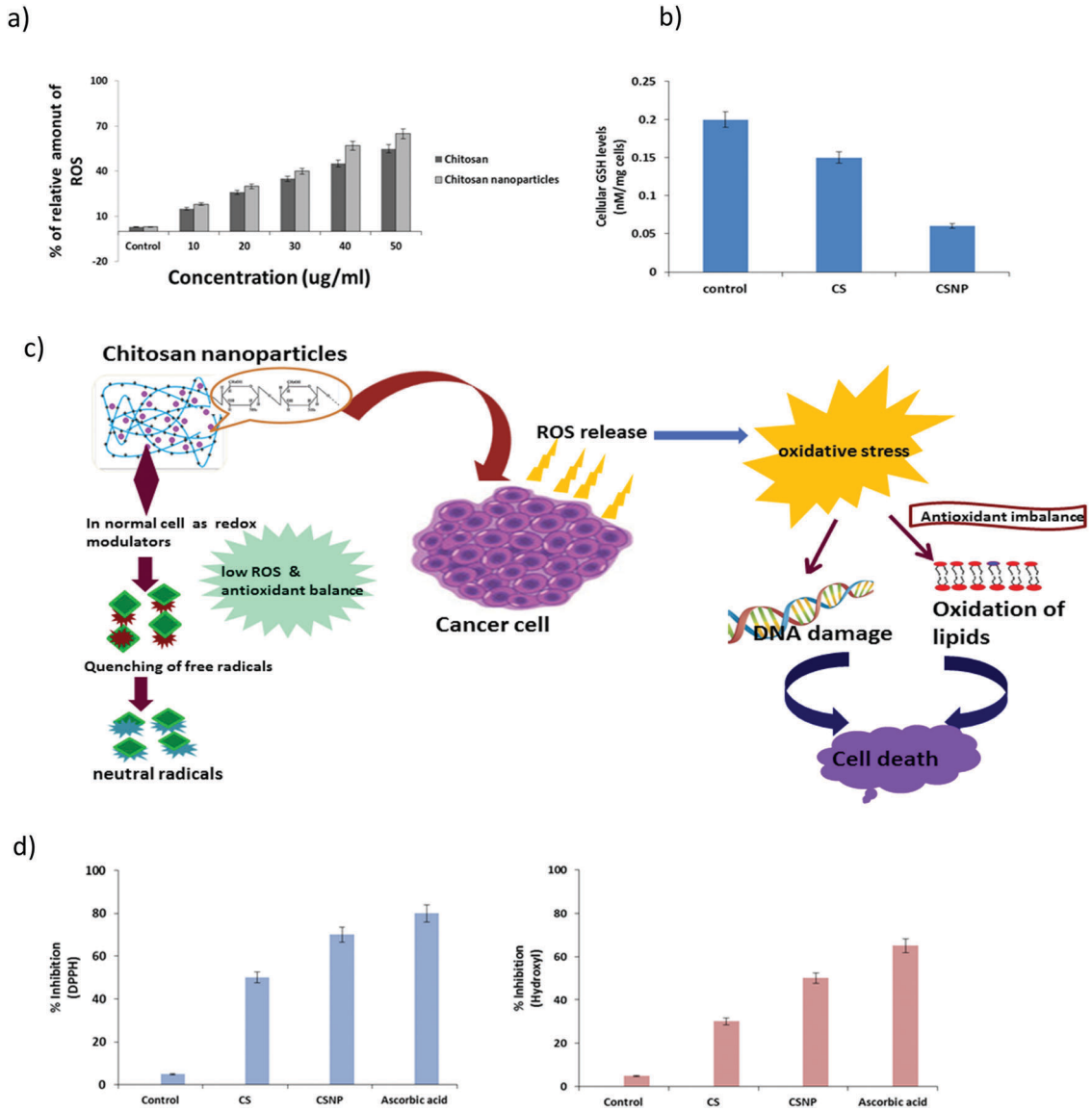

Fig. 7 The effect of chitosan nanoparticles in ROS production and antioxidant capacity. (a) The percentage of reactive oxygen species released as an indicator of cell death. (b) The cellular GSH levels and (c) mechanism of chitosan nanoparticle induced ROS mediated cytotoxicity. (d) Antioxidant activity (% scavenging) analyzed by DPPH assay and hydroxyl scavenging activity. Data are represented as the mean value ± S.D. of three independent replicates (n = 3). (* indicates a significant difference ($p < 0.05$) compared to the control.)

Antiproliferative activity/live dead cell staining

The apoptotic index induced by chitosan and chitosan nanoparticles was quantified using calcein and propidium iodide staining. The intracellular esterase in live cells converts cell permeable non-fluorescent calcein dye to fluorescent calcein dye, hence allowing the assessment of cell viability. On the other hand, propidium iodide is impermeable to the intact cell membrane of viable cells but it is able to enter dead cells with a porous membrane to intercalate with the nucleic acid to give a fluorescence signal, allowing the assessment of cell death.[28]

When cells are incubated with 50 μg mL^{-1} of chitosan or 50 μg mL^{-1} CSNPs, the number of propidium iodide cells increased (shown in Fig. 6). This result shows that chitosan and CSNPs are cytotoxic to acute lymphoblastic leukemia cells, causing apoptosis and cell death. The morphology of the cells after 4 hours of CSNP treatment was examined. The shrinkage of the cells with membrane blebbing and nuclear fragmentation in the Jurkat cells stained red is characteristic of an apoptotic cell which leads to cell death while the viable cells stained green are more spherical in shape. These results suggest that the chitosan nanoparticles exhibited a cytotoxic

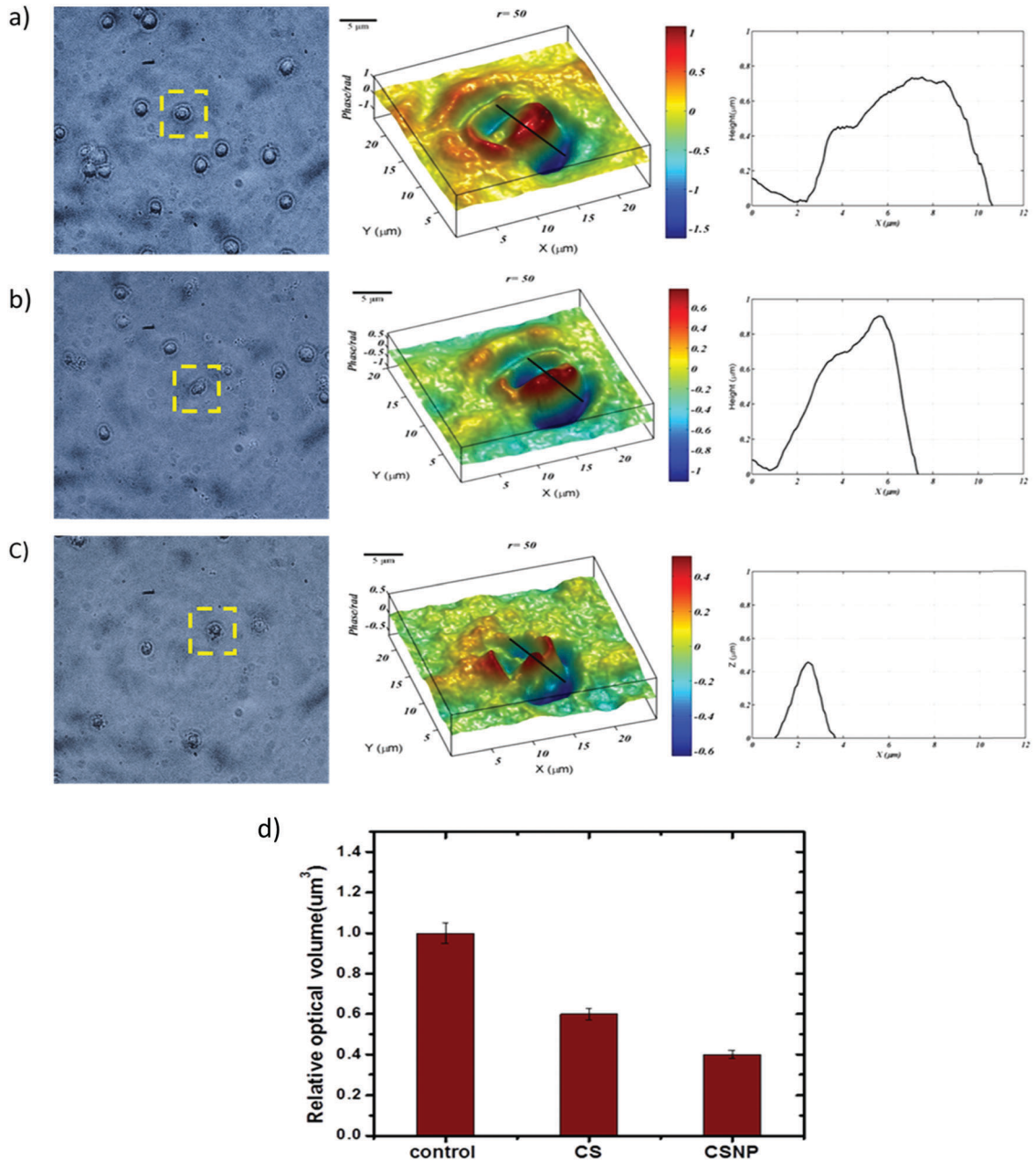

Fig. 8 (a–c) Phase imaging (40× magnification) of acute lymphoblastic leukemic cells for changes in cell behaviour: (a) the control cells, (b) chitosan treated cells & (c) chitosan nanoparticle treated cells and the (d) relative optical volume change in leukemia cells with chitosan and chitosan nanoparticles. Data are represented as the mean value ± S.D. of three independent replicates (n = 3).

effect by decreasing the viability of cells more significantly than chitosan. Therefore, the chitosan nanoparticles first adsorbed onto the negatively charged tumor cell membrane by electrostatic interaction[29], then they exhibited cytotoxic effects by damaging the membrane and disrupting the organelle, and finally this led to cell death as the structure broke down.

Intracellular reactive oxygen species & total cellular GSH

Measurement of intracellular reactive oxygen species (ROS) plays a vital role in understanding the progression of the disease. Acute lymphoblastic leukemia cells incubated with the chitosan nanoparticles showed a depletion in GSH with a significant increase in the production of intracellular ROS when compared to the control (shown in Fig. 7a and b). At higher concentrations the treated cells showed a remarkable increase in the level of ROS which likely reveals that most cells underwent a decrease in the intracellular antioxidant capacity. Oxidants or stimulators of cellular oxidative metabolism are the agents that induce apoptosis, and some agents which inhibit apoptosis exhibit antioxidant activity.[30] These reactive oxygen species may lead to cellular transformation and tumorigenesis. When there is a rapid increase of ROS in cancer cells this makes the cell more vulnerable to exogenous factors causing irreversible cellular damage.[31] The ROS has been implicated as a second messenger in multiple signaling pathways and can also play an important role in apoptosis by regulating the activity of certain enzymes involved in the cell death pathway.[32] Cytotoxicity and ROS generation by chitosan nanoparticles indicate that ROS production probably causes apoptotic cell-death *via* the antioxidant imbalance and oxidative stress mechanism. This selective induction of cytotoxicity in cancer cells is a promising therapeutic strategy to kill cancer cells without affecting normal cells.

Radical scavenging activity

Antioxidant activity was determined by DPPH and hydroxyl radical scavenging which is quantified in terms of the inhibition percentage of the pre-formed free radical by the antioxidants (shown in Fig. 7d), and the EC_{50} (concentration required to obtain a 50% antioxidant effect) is a typically employed parameter used to express the antioxidant capacity and to compare the activity of the compounds. The radical scavenging activity of chitosan nanoparticles may be attributed, due to the hydroxyl and amine groups, to quenching of the free radicals.[33] The free radical scavenging activity of chitosan nanoparticles was evaluated by comparing its inhibitory activity on the formation of DPPH and hydroxyl radicals. The observed increase of free radical scavenging activity suggests that chitosan nanoparticles have an efficient protective mechanism in response to the basal ROS in normal cells which may help regeneration under oxidative stress conditions.[33]

Changes in cellular phenotype

Cell death can be characterized by a distinct set of temporal, morphological, biochemical and gene expression features in apoptosis, necrosis and autophagy. Intrinsic physical features, in particular volume changes, thickness and size, accompany cell death processes and are often used to define the different cell death pathways.[34] To understand the individual cell level dynamic phenotypes in cancer cell proliferation in response to treatment, phenotype changes in acute lymphoblastic leukemia cells treated with chitosan and chitosan nanoparticles were detected using a (d'Biomager) phase imaging system. A quantitative phase image of the cells was obtained *via* numerical analysis. The results show that the average area and optical volume of the chitosan nanoparticle treated cells are significantly reduced when compared with that of the chitosan treated and control cells, which reveals the cytotoxic effect of the chitosan nanoparticles on the cancer cells.

In the present study the phenotype analysis of the acute lymphoblastic leukemic cells, both the control and treated cells, is demonstrated in Fig. 8(a–c). The control cells have a uniform shape which indicates that the cells are in a healthy state. Meanwhile the treated cells, due to cell death, gradually become irregular as a result of the surface tension of the solution. In the treated cells, not only does the surface area change but the cell thickness also has a visible change. The oversized optical thickness and change in surface area and volume is characteristic of abnormal cells.[35] The relative optical volume changes can be used to differentiate the cell metrics and to determine the influence of the drugs. Changes in growth and cell proliferation rate can be measured *via* the combinatorial use of cell dry mass and thickness measurements.[36] The increase in low optical thickness with the chitosan nanoparticle treated cells is consistent with increasing cell death. With these results, we can demonstrate that the cells treated with chitosan

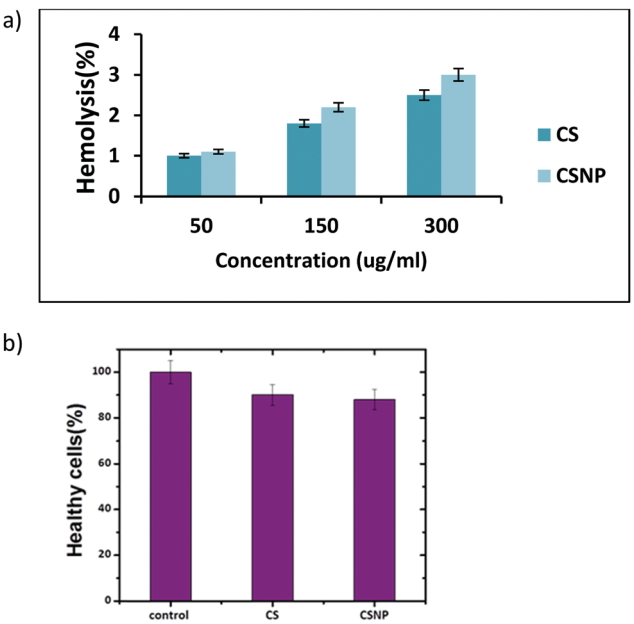

Fig. 9 Hemocompatibility. (a) The percentage of hemolysis for chitosan and chitosan nanoparticles. (b) Quantification of healthy cells derived from the morphology of RBCs with chitosan and chitosan nanoparticles. Data are represented as the mean value ± S.D. of three independent replicates (n = 3).

nanoparticles have an obvious change in the cell phenotype. The size distribution between the control and the treated cells in both the cell area and optical volume supports this change. The phenotypic changes observed confirm the significant difference in the area of the cells in the chitosan nanoparticle treated cells and that of the chitosan and control cells. This indicates that chitosan nanoparticles at a concentration of 50 μg mL^{-1} could cause cellular shrinkage and nuclear fragmentation which implies that they could influence the process of cell death. In addition, the changes in optical volume and thickness in the treated cells support this effect of cytotoxicity and warrants further investigation.

Hemocompatibility of chitosan and chitosan nanoparticles

Measurement of free hemoglobin is a direct method for determining the hemolytic index[37] of the nanoparticles tested.

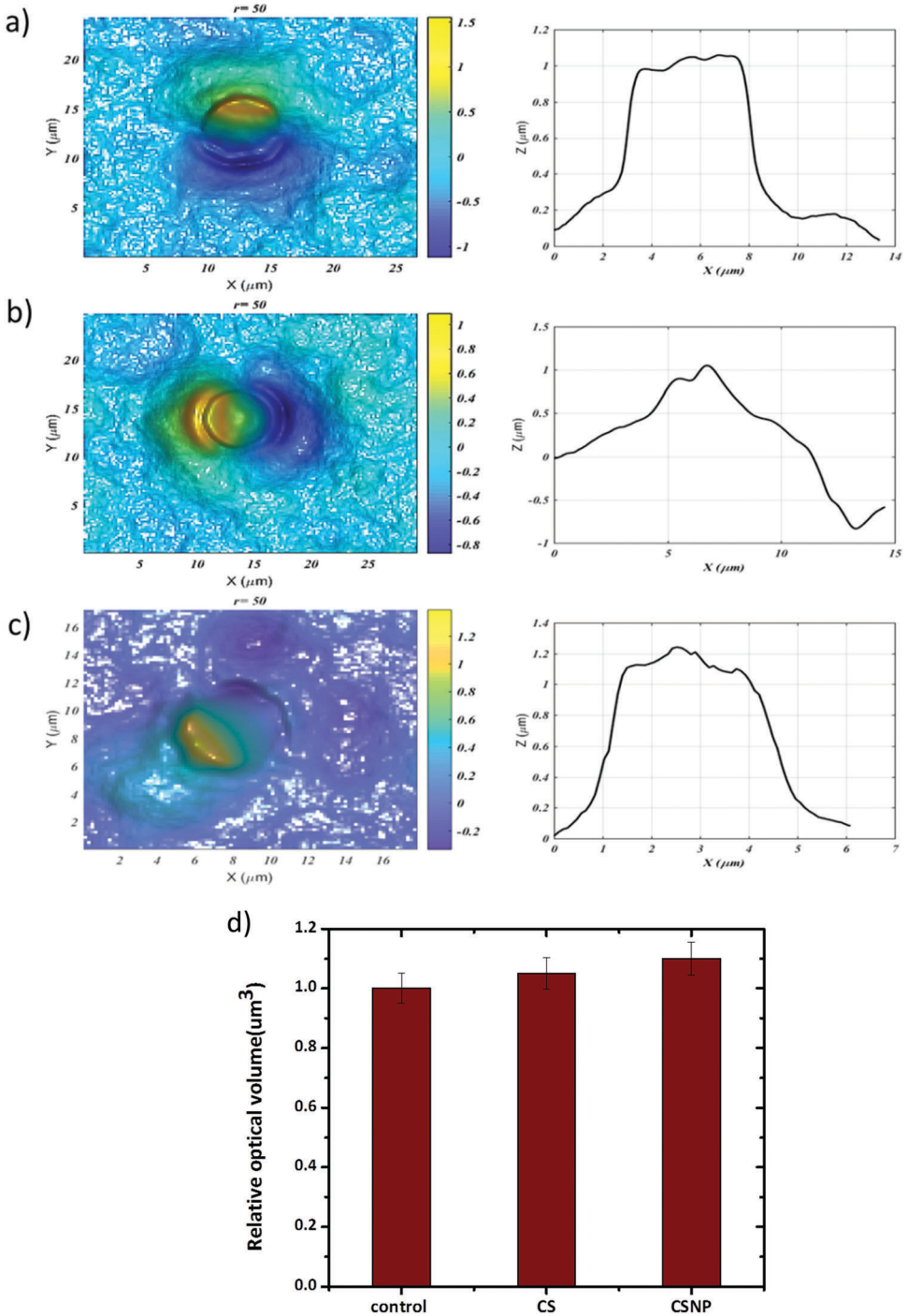

Fig. 10 Phase imaging (40× magnification) of RBCs – (a) control cells, (b) chitosan treated cells & (c) chitosan nanoparticle treated cells. (d) The relative optical volume change in RBCs with chitosan and chitosan nanoparticle. Data are represented as the mean value ± S.D. of three independent replicates (n = 3).

Our results showed that the percentage of hemolysis both by chitosan and chitosan nanoparticles was comparatively less than that for the positive control indicating that they are non-hemolytic as this falls within the range of 0–2%, which is considered to be non-hemolytic as per the ASTM standard. The hemolytic degree of the positive control was 100% and for the negative control the cells showed 0% lysis. With an increasing concentration of chitosan and chitosan nanoparticles the hemolytic degree increased with a maximum hemolytic degree of 3.0% (shown in Fig. 9). Therefore the hemolytic degree is lower than the permissible limit of 5% for biomaterials in contact with blood.[38] The morphological analysis of RBCs showed neither significant deformation nor aggregation when treated with chitosan and chitosan nanoparticles revealing excellent hemocompatibilty (Fig. S4, ESI†). Together these results demonstrate that chitosan nanoparticles are non-toxic, and do not initiate the process of oxidation in the cell membrane, and therefore these nanoparticles can be safely applied to intravenous systems as well as in therapeutic applications.

The hemocompatibility of the synthesized chitosan nanoparticles and the chitosan polymer towards RBCs was evaluated by quantitative phase imaging by analyzing the intrinsic physical features, in particular volume changes, thickness and size, that provide quantitative information on the cell death mechanism to monitor the extent of toxicity. Quantitative phase detection is a non-invasive imaging alternative to measure the behavioral changes of the living cells in real time.[39] Results show that the average area and optical volume of the chitosan and chitosan nanoparticle treated RBCs do not show much alteration when compared with those of the control cells (shown in Fig. 10). From the results it can also be determined that the synthesized nanoparticles and the chitosan polymer are sufficiently hemocompatible for *in vivo* applications suggesting that these nanoparticles are biocompatible candidates for use as drug targeting agents or theranostics that are injected intravenously.

Conclusion

In summary, chitosan nanoparticles with a positive surface charge selectively induce cytotoxicity in leukemia cells by targeting the oxidative stress mechanism. Redox directed agents which enhance oxidative stress in cancer cells are considered to be potential antineoplastic agents. Chitosan nanoparticles induced selective cytotoxicity by depleting glutathione and increasing ROS. The detection of cell death *via* quantitative phase measurement also validates the results obtained from various assays and confirms chitosan nanoparticles as potential drug candidates. The low hemolytic activity makes them a promising candidate for designing intravenous applications. Therefore, the synthesized novel chitosan nanoparticles can be considered as an important polymer for redox active drugs and warrant further investigation for the benefit of mankind and they can also considered for different biomedical applications. Taking into account the natural origin and biocompatibility, without lethal toxicity to RBCs, chitosan nanoparticles would be a safe and efficacious candidate suitable for a wide spectrum of prophylactic and therapeutic vaccines, for which a balanced and potent stimulation of both the cellular and humoral responses is required.

Author contributions

S. S. conceived the study. S. S. and N. Y. K. carried out the experiments, and S. S. analyzed the results. R. E. and A. P. carried out the phase imaging experiment and analyzed the results. S. S. wrote the manuscript. Advice and approval was given by A. A. & M. J. L.

Conflicts of interest

The authors declare that they have no competing interest.

Acknowledgements

This research was supported by the National Research Foundation, Singapore, through the Singapore MIT-Alliance for Research and Technology's Biosystems and Micromechanics (BioSyM) IRG research program. The authors thank Prof. Peter Praiser (NTU) and Dr Smitha (Biosym) for providing us with the RBC sample.

References

1 S. Caban, Y. Capan, P. Couvreur and T. Dalkara, *Neurotrophic Factors: Methods and Protocols*, 2012, pp. 321–332.
2 S. Chandra, N. Chakraborty, A. Dasgupta, J. Sarkar, K. Panda and K. Acharya, *Sci. Rep.*, 2015, 520–530.
3 E. I. Rabea, M. E. T. Badawy, C. V. Stevens, G. Smagghe and W. Steurbaut, *Biomacromolecules*, 2003, **4**, 1457–1465.
4 V. Zargar, M. Asghari and A. Dashti, *ChemBioEng Rev.*, 2015, **3**, 204–236.
5 L. Qi and Z. Xu, *Bioorg. Med. Chem. Lett.*, 2006, 164243.
6 L. Qi, Z. Xu and M. Chen, *Eur. J. Cancer*, 2007, **43**, 184–193.
7 M. J. Masarudin, S. M. Cutts, B. J. Evison, D. R. Phillips and P. J. Pigram, *Nanotechnol., Sci. Appl.*, 2015, **8**, 67–80.
8 H. Katas and H. O. Alpar, *J. Controlled Release*, 2006, **115**, 216–225.
9 T. Wang, J. Bai, X. Jiang and G. U. Nienhaus, *ACS Nano*, 2012, **6**, 1251–1259.
10 D. Jeevitha and K. Amarnath, *Colloids Surf., B*, 2013, **101**, 126–134.
11 A. Kummrow, M. Frankowski, N. Bock, C. Werner, T. Dziekan and J. Neukammer, *Cytotherapy*, 2013, **83A**, 197–204.
12 X. Zheng, Y. Zhang, F. Yin, X. Xiong, Z. Gong, B. Zhu, P. Lu and P. Xu, *Carbohydr. Polym.*, 2016, **84**, 1048–1050.
13 M. Forkink, J. M. Smeitink, R. Brock, P. M. Willems and W. H. Koopman, *Biochim. Biophys. Acta*, 2010, **1797**, 1034–1044.
14 M. S. Moron, J. N. De Pierre and V. C. Mannervik, *Biochem. Biophys. Acta*, 1979, **582**, 67–68.
15 Y. Niu, D. Ke, Q. Yang, X. Wang, Z. Chen, X. An and X. Shen, *Food Chem.*, 2012, **135**, 1377–1382.

16 K. Elizabeth and M. N. A. Rao, *Int. J. Pharm.*, 1990, **58**, 237–240.
17 Z. Ren, G. Chen, Z. Wei, L. Sang and M. Qi, *J. Appl. Polym. Sci.*, 2013, **127**, 308–315.
18 d'Optron Pte Ltd, http://www.doptron.com.
19 Y. Xu and Y. Du, *Int. J. Pharm.*, 2003, **250**, 215–226.
20 F. Danhier, O. Feron and V. Préat, *J. Controlled Release*, 2010, **148**, 135–146.
21 H. Zhang, J. Jung and Y. Zhao, *Carbohydr. Polym.*, 2016, **137**, 82–91.
22 S. W. Ali, S. Rajendran and M. Joshi, *Carbohydr. Polym.*, 2011, **83**, 438–446.
23 X. Jia, X. Chen, Y. Xu, X. Han and Z. Xu, *Carbohydr. Polym.*, 2009, **78**, 323–329.
24 J. Zhang, X. G. Chen, W. B. Peng and C. S. Liu, *Nanomedicine*, 2008, **4**, 208–214.
25 U. O. Hafeli, J. S. Riffle, L. Harris-shekhawat, A. Carmichael-baranauskas, F. Mark and J. P. Dailey, *Mol. Pharmaceutics*, 2009, **6**, 1417–1428.
26 S. Mitra, U. Gaur, P. C. Ghosh and A. N. Mitra, *J. Controlled Release*, 2001, **74**, 317–323.
27 G. Unsoy, S. Yalcin, R. Khodadust, G. Gunduz and U. Gunduz, *J. Nanopart. Res.*, 2012, **14**, 964.
28 I. Ksiazek, K. Sitarz, M. Roslon, E. Anuszewska, P. Suchocki and J. D. Wilczynska, *Cancer Genomics Proteomics*, 2013, **10**, 225–232.
29 C. Schult, M. Dahlhaus, S. Ruck, M. Sawitzky, F. Amoroso, S. Lange, D. Etro, A. Glass, A. Fuellen, S. Boldt, O. Wolkenhauer, L. Neri, M. Freund and C. Junghanss, *BMC Cancer*, 2010, **10**, 1–11.
30 E. J. Chung, S. G. Hwang and P. Nguyen, *et al.*, *Blood*, 2002, **3**, 982–990.
31 D. A. Zaharoff, C. J. Rogers, K. W. Hance, J. Schlom and J. W. Greiner, *Vaccine*, 2007, **25**, 2085–2094.
32 A. Aranda, L. Sequedo, L. Tolosa, G. Quintas, E. Burello, J. V. Castell and L. Gombau, *Toxicol. In Vitro*, 2013, **27**, 954–963.
33 M. Negrette-Guzmán, S. Huerta-Yepez, E. Tapia and J. Pedraza-Chaverri, *Free Radical Biol. Med.*, 2013, **65**, 1078–1089.
34 S. Son, A. Tzur, Y. Weng, P. Jorgensen and J. Kim, *et al.*, *Nat. Methods*, 2012, **9**, 910–912.
35 M. Mir, Z. Wang, Z. Shen, M. Bednarz and R. Bashir, *et al.*, *Proc. Natl. Acad. Sci. U. S. A.*, 2011, **108**, 13124.
36 C. Gorrini, S. Harris and T. W. Mak, *Nat. Rev. Drug Discovery*, 2013, **12**, 931–947.
37 Y. Zhao, S. Wang, Q. Guo, M. Shen and X. Shi, *J. Appl. Polym. Sci.*, 2013, **127**, 4825–4832.
38 A. Neamnark, N. Sanchavanakit, P. Pavasant, T. Bunaprasert, P. Supaphol and R. Rujiravanit, *Carbohydr. Polym.*, 2007, **68**, 166–172.
39 A. Barty, K. A. Nugent, D. Paganin and A. Roberts, *Opt. Lett.*, 1998, **23**(11), 817–819.

